Influence of emitter-receiver number on measurement accuracy in acoustic pyrometry

Lorenzo Ferrari*, *Gianluca* Caposciutti, *Gianluca* Pasini, *Guido Francesco* Frate, *Umberto* Desideri

University of Pisa, Department of Energy, Systems, Territory and Construction Engineering (DESTeC)
Largo Lucio Lazzarino, 1, 56122 – Pisa – Italy

Abstract. Acoustic pyrometry is an interesting technique that may find several useful applications in turbomachinery. As the speed of sound is directly related a medium temperature, this measurement technique estimates the temperature of a gas by considering the time of flight of an acoustic wave moving through it. If only an acoustic emitter-receiver couple is used, only the average temperature along the acoustic path can be determined. If multiple emitter-receiver couples laying on the same plane are used, a reconstruction of the temperature map in the section is possible. This estimation is performed by considering that multiple acoustic paths travel across the same sub-portions of the section and, therefore, the temperature of each sub-portion affects the time of flight along several sound paths. Many parameters affect the accuracy of the measurement, and they are related to the physic of the phenomena involved in the measurement, the accuracy of the instrumentation used, the interaction between the acoustic wave and the flow velocity and the hardware set-up. In this study, the impact of some set-up parameters on the accuracy of the measurement was investigated and, in particular, the number of sound emitter-receiver couples and the number of investigation sub-portions in which the section is divided. A reference temperature map has been considered as a benchmark. This study, which is a preliminary investigation on this technique, was useful to assess the capability of this methodology to correctly describe a temperature distribution in an ideal condition. Therefore, it represents a first step in the set-up of an experimental investigation with an acoustic pyrometer..

1 Introduction

Many situations in turbomachinery require the measurement of a gas temperature over a large section to assess the correct operation of components (e.g. boilers, heat recovery steam generators, turbine discharge ducts or combustion chambers). This measurement is generally performed by adopting a rake of thermocouples and may be very intrusive if a detailed temperature profile estimation is required [1].

An increasing interest is being paid to acoustic pyrometry as it allows the estimation of a temperature distribution in a section with virtually no interactions with the flow. In addition, this technique does not rely on the achievement of a thermal equilibrium between a sensing element and the flow and therefore is not affected by measurement lags due to the thermal inertia of the sensor. Acoustic pyrometry is based on the measurement of the time of flight of an acoustic wave as the propagation speed of the wave is directly related to medium temperature. If only an acoustic emitter-receiver couple (ERC) is used, only the average temperature along the acoustic path can be determined. If multiple emitter-receiver couples laying on the same plane are used, a reconstruction of the temperature map in the section is possible.

This estimation is performed by considering that multiple acoustic paths travel across the same sub-portions of the section and, therefore, the temperature of each sub-portion affects the time of flight along several sound paths. The measurement is generally performed by using an emitter devices which generates an intense sound signal in a short time window. The receivers placed in the same section detect the incoming signal, and the time required to travel from the emitter to the receivers is estimated.

As the temperature of the fluid increases, the time of flight of an acoustic wave decreases and, for a fixed emitter-receiver, the estimation of the time of flight becomes more and more critical (smaller time difference). Therefore this technique is particularly suitable for measuring the temperature distribution on large diameter ducts when the temperatures are medium-low. This is the reason why this technique has been adopted in the past for the temperature measurement in industrial or power plant boilers [1,2,3] or furnaces [4].

More recently, this technique has been used in turbomachinery applications for the determination of the exhaust gas temperature map of a heavy duty industrial gas turbine [5,6] and the dynamic measurement of entropy waves in a combustor [7].

Many errors may affect the accuracy of the temperature measurement. These may be identified as problems related to the estimation of the gas physical

* Corresponding author: lorenzo.ferrari@unipi.it

parameters, the path length and the time of flight. Potential error sources are:

1. The method adopted to detect the arrival of the acoustic wave and the sampling frequency used to determine the time of flight. These parameters may be particularly critical in the case of noisy environments. Typically, sampling rate around 1 MHz [8] and complex sound emission are used [6]
2. Physical properties of the gas that are not uniform or far from those of an ideal gas (the assumption of an simple relation between the temperature and the speed of sound is no more valid)
3. The presence of a strong temperature gradient can lead to curved acoustic path thus leading to a wrong estimation of the distance travelled by the acoustic wave [2]
4. If the flow velocity is not negligible in comparison to the speed of sound, the composition of the two velocities may lead to a wrong estimation of the time of flight
5. The measurement set-up (i.e. the number of ERCs and their position and the number of cells and their geometry) the may lead to relevant errors in the estimation of the temperature distribution

This study is mainly focused on the last of the previous bullet points. In particular, the impact on the temperature estimation accuracy of the number of sound ERCs and the number of investigation sub-portions in which the section is divided have been investigated. A reference temperature map has been considered as a benchmark. This study was useful to assess the capability of this technique to correctly describe a temperature distribution in an ideal condition and represents a first step in the set-up of a measurement with this technique.

2 Elements of acoustic pyrometry

The propagation speed of an acoustic wave depends on the characteristics of the medium and, in particular, its temperature. This is of course valid locally. If zones with different temperatures are encountered during the travel, the local speed of sound will change accordingly, thus affecting the time of flight between the two points. Acoustic pyrometry is based on this concept. An emitter generates a sound input which propagates up to a receiver at a known distance. The time flight is recorded and used to calculate the velocity along the sound path. If the sound path is supposed to be dived in sub-portions, the speed of sound in each sub-portion may be expressed as:

$$a_i = \sqrt{kRT_i}$$

Therefore, the time of flight along a sound ray may be written as:

$$\tau = \sum \frac{l_i}{a_i}$$

where l_i is the sound ray length in the section sub-portion. If multiple couples of emitters and receivers are used, several sound rays will come across the same section and the different time of flight may be used to compute the temperature distribution. Several methods exists to perform this operation. In this study that proposed by [9] and [10] is used. The reader is advised to refer to those studies for further details on the computational procedure. A synthesis of the conceptual passages is reported here, for the sake of clarity:

1. The region is divided in cells where the temperature is assumed as a constant. A guess temperature distribution is assumed
2. The time of flight between the ERCs is calculated by taking into account the sound ray path and the temperature in the cells where it pass through
3. The difference between the measured and estimated times of flight along a sound rays is calculated and used to update the guess temperature distribution
4. A very weak smoothing procedure is used to average the value in each cell with those of the adjacent cells. This correction method is applied to consider that high temperature gradient are physically unfeasible in a flow.
5. Steps from 2 to 4 are repeated until convergence is achieved on the difference between the estimated and measured time of flight.

According to [9] a SIRT (Simultaneous Iterative Reconstruction Technique) procedure was used to calculate the correction to the temperature map in each iteration step.

CASE STUDY

As a case study, a duct with a square section of 1m^2 and a temperature distribution as in Figure 1 was considered. The chosen distribution was purposely selected to be simple to have a prompt detection of the reconstruction capability of the methodology adopted. For the purpose of the analysis each emitter was also considered as a potential receiver. Even though in an actual application they might not be perfectly located in the same place, this potential shift was neglected for the sake of simplicity. A variable number of ERC was considered ranging from 3 to 15 couples per side.

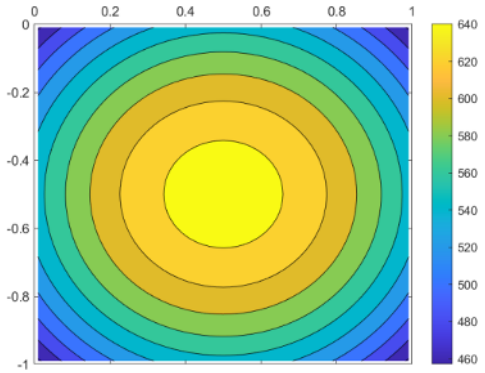

Figure1. Temperature reference map (K).

Typical applications of this technique generally use a limited number of ERCs to keep the costs low and reduce the system complexity. Nevertheless, this range of ERCs was chosen to explore the reconstruction capability of this technique in a wide range of combinations. By increasing the number of ERCs, also the number of sound rays increases. According to the theory proposed by [9] the number of cells should be

less or equal than the number of sound rays. In this study, only cells with a square geometry were considered. The corresponding number of cells per side according to the number of ERCs per side is reported in Table 1. In Table 1, the maximum and minimum number of sound ray segments per cell is also reported for each configuration.

Table 1. Number of sound rays, nominal cells per side and maximum and minimum number of segments per cell according to the number of ERCs per side.

ERCs per side	Sound rays	Cells per side	Seg. (max)	Seg. (min)
3	28	5	8	3
4	66	8	14	4
5	120	10	19	6
6	190	13	27	9
7	276	16	36	8
9	496	22	53	10
12	946	30	82	14
15	1540	39	116	16

According to the computation methodology a reference time of flight for each ERCs is necessary. This time of flight would come from a hypothetical measurement of the selected temperature map. To estimate this quantity, a very fine mesh was considered and the average temperature in each cell was calculated. During the simulations, the time of flight for each sound rays was calculated by considering this set of cells and temperature values and was assumed as the "measured" time of flight.

3 Results

As described above, the computation of the temperature is based on an iterative procedure that starts from a random distribution of temperatures (one temperature value for each cell). As a stop criteria for the iteration, two parameters were considered:

1. The maximum of the absolute value of the time of flight error over all the sound paths. As a stop condition a value below 10^{-8} is imposed
2. The difference of the previous parameter between two subsequent iterations. As a stop condition a value below 10^{-16} is imposed

The second condition was included to guarantee a safe stop of the iteration procedure. In many cases, the iteration achieved a stalling point (around 10^{-7} or 10^{-6} and was not able to further reduce the error (first condition).

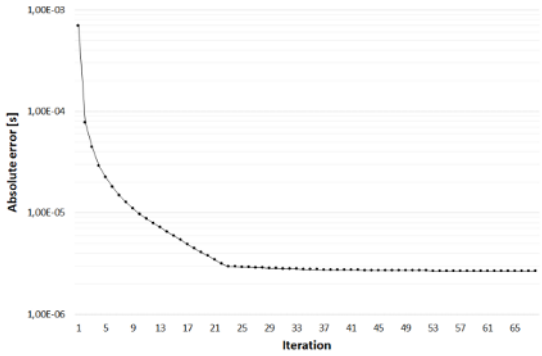

Figure 2. Maximum value of the difference between the correct and the estimated times of flight among all the sound rays (absolute value).

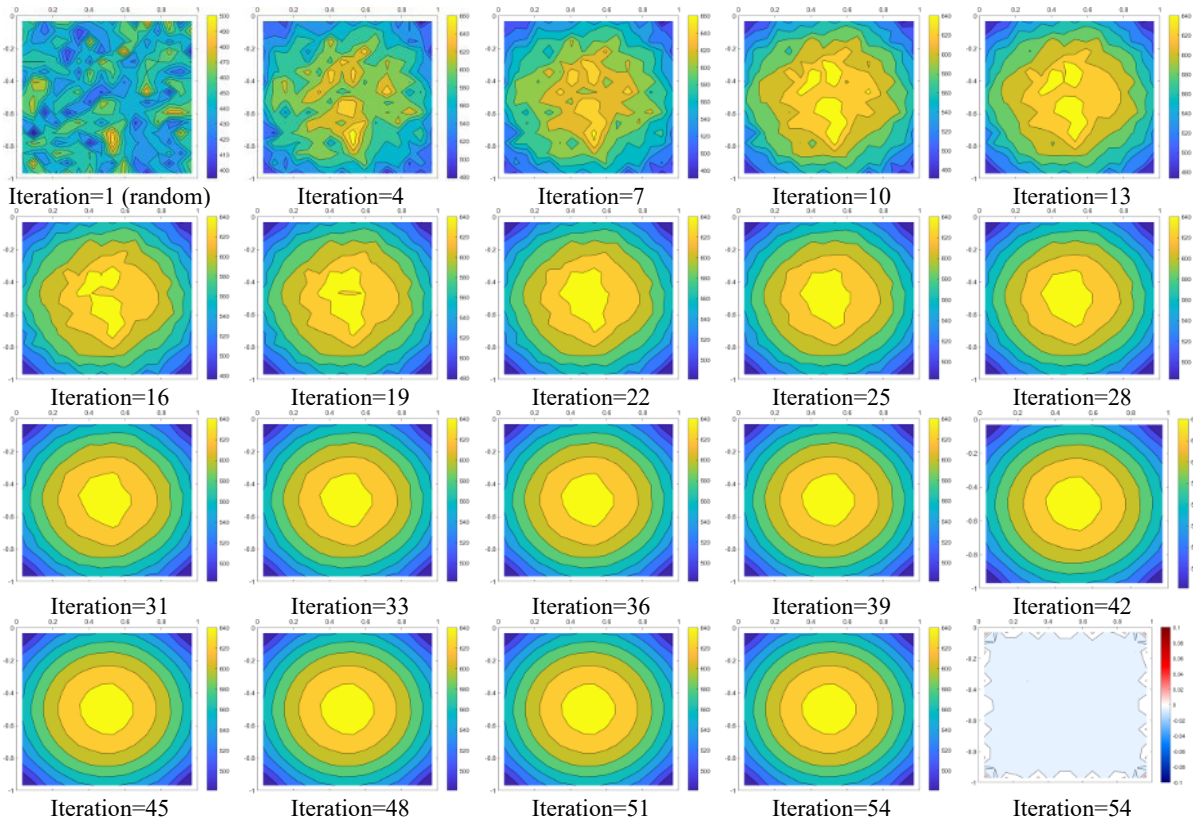

Figure 3. Temperature map in the first 54 iterations and % error at the 54th iteration (7 ERCs, 16 cells per side).

The main reason for this, might be ascribed to the nature of the problem. The correctness of the temperature estimation during the iteration process is performed by computing the overall time of flight along a sound path and comparing it with that obtained from the measurement. The temperature map is then corrected according to this difference. This quantity is dependent on all the contributions provided by the cells which the sound ray passes through. Therefore a small uncertainty on the overall time of flight may still be present even though the error on cell temperatures are low. In any case, the reconstruction accuracy was very satisfactory as shown further below. As an example, in Figure 2, the absolute value of the maximum difference between the estimated and the correct times of flight is reported for each iteration up to convergence. In Figure 3 the sequence of temperature maps during the iteration procedure is reported. By starting from a random temperature distribution, the procedure modifies the temperature values in the cells to match the times of flight and quickly achieves a temperature map that is very similar to the expected one. In Figures 4-6, the sound ray paths, the cells distribution, the reconstructed temperature map and the percentage error distribution are reported when using 3, 5 and 7 ERCs per side. The strong impact of this parameter on the accuracy of the reconstructed temperature map is clear. When the number of ERCs is low, the accuracy of the temperature estimation is limited by both the number of sound rays and the dimension of the estimation cells..

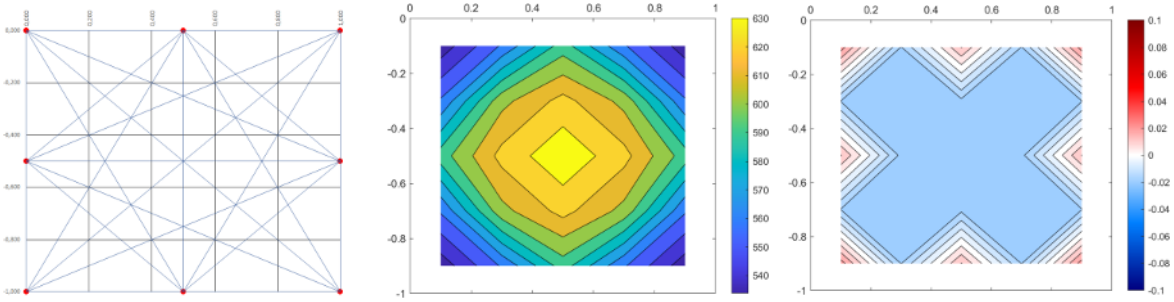

Figure 4. Sound rays, reconstructed temperature map and % error with 3 ERCs per side.

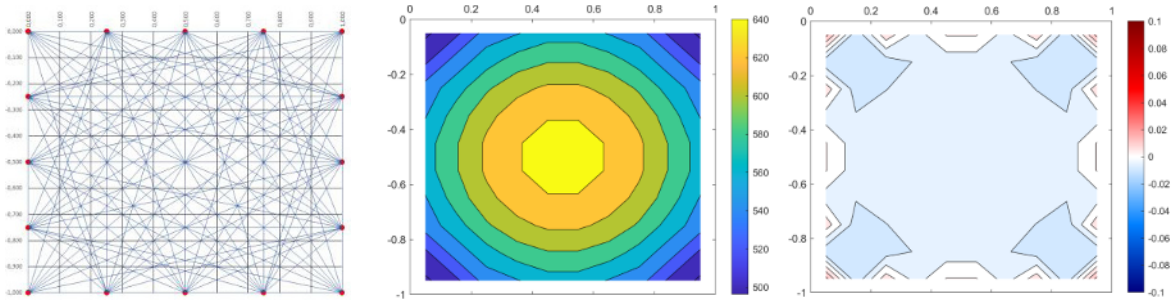

Figure 5. Sound rays, reconstructed temperature map and % error with 5 ERCs per side.

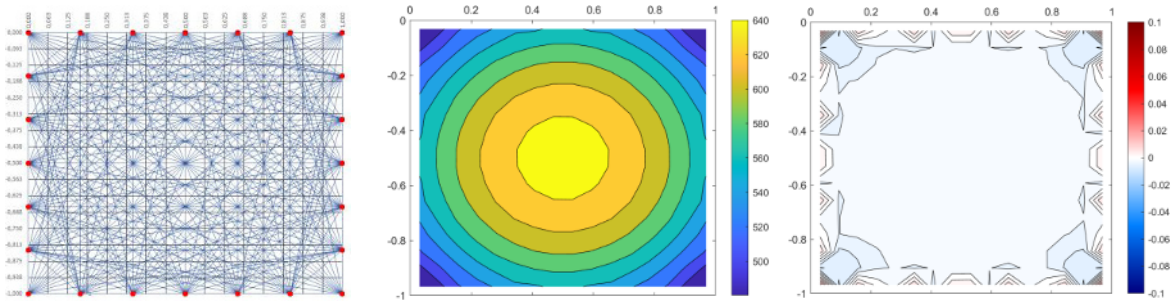

Figure 6. Sound rays, reconstructed temperature map and % error with 7 ERCs per side.

7	4	8	4	7
4	4	3	4	4
8	3	4	3	8
4	4	3	4	4
7	4	8	4	7

15	8	19	12	14	14	12	19	8	15
8	8	9	8	10	10	8	9	8	8
19	9	6	7	9	9	7	6	9	19
12	8	7	6	10	10	6	7	8	12
14	10	9	10	7	7	10	9	10	14
14	10	9	10	7	7	10	9	10	14
12	8	7	6	10	10	6	7	8	12
19	9	6	7	9	9	7	6	9	19
8	8	9	8	10	10	8	9	8	8
15	8	19	12	14	14	12	19	8	15

23	12	30	20	19	35	21	25	25	21	35	19	21	31	12	23
12	8	13	13	14	13	15	15	15	15	13	14	15	15	8	12
30	13	12	12	13	11	14	14	14	14	11	13	13	13	14	31
20	13	12	13	12	12	14	13	12	13	12	12	13	12	14	21
19	14	13	12	11	11	12	11	11	12	11	11	12	13	14	19
36	14	11	12	13	12	12	17	17	12	11	12	12	11	14	36
21	15	14	13	13	12	13	14	13	12	12	13	13	14	16	22
25	15	15	13	11	16	13	11	11	13	17	12	12	14	15	25
25	15	14	12	11	16	13	11	11	13	16	11	12	14	15	25
22	16	14	13	15	14	12	13	14	13	11	12	13	14	15	21
36	14	11	12	13	12	11	16	17	12	10	11	12	11	13	35
19	14	13	12	12	12	13	12	11	12	11	11	12	13	15	20
21	14	12	13	12	12	13	12	12	13	12	12	13	12	13	20
31	14	13	13	13	11	14	14	15	15	11	13	13	13	13	30
12	8	14	14	14	13	15	15	15	15	13	14	14	14	8	12
23	12	31	21	19	35	21	25	25	21	36	20	21	31	12	23

Figure 7. Number of segments for each cell in case of 3, 5 and 7 ERCs per side (5, 10, 16 cells per side).

The resulting temperature map is coarser and the errors becomes greater, even though they are still limited in average terms. In more detail, the methods is not able to estimate correctly the temperature gradients close to the walls and a general underestimation of the temperature is observed in the central region. By increasing the number of ERCs the estimation capability of the systems improves greatly

To investigate further the impact of the number of ERCs, the number of sound ray segments in each cell in the case of 3, 5 and 7 ERCs per side has been reported in Figure 7. In this figure the geometric proportion of the cells is also respected. As the time of flight along a sound rays is computed by considering the sum of the times of flight within each cell through which it passes, the number of segments in each cell is an indication of the number of time the temperature of a cell is considered in the estimation of the temperature map. It is easy to understand that the lower the number of segments, the lower is the accuracy in the estimation. Of course, if the number of segments in a cell is zero, the estimation of the temperature in that cell is not possible.

In Figure 8, the average error in the estimation of the temperature and the standard deviation range is reported for an increasing number of ERCs. The number of cells in each analysis is that reported in Table 1. The impact of the number of ERCs on the accuracy of the measurement is apparent. Since the complexity of the measurement increases with the number of ERCs, a tradeoff between accuracy and feasibility should be chosen. From the results of the this analysis, a number of ERCs between 5 and 7 turned out to provide very accurate results with a limited system complexity. In addition, it is interesting to notice that the average error tends to be always in the negative semi-plane for every number of ERC (even though it became very small over 9 ERCs).

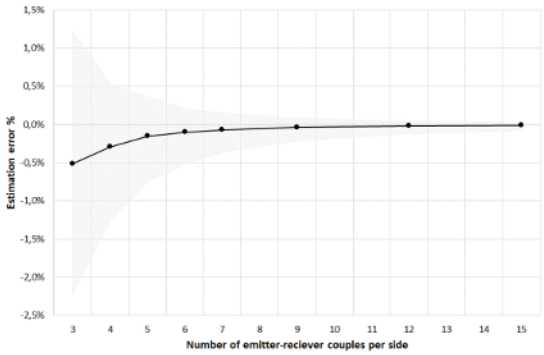

Figure 8. Relative error in the temperature distribution vs the number of ERCs per side.

In Figure 9, the average number of segments per cell and the standard deviation range is reported for different values of ERCs. By increasing the number of ERCs the number of segments per cell increases linearly. The good results achieved for an ERC number between 5 and 7 correspond to an average number of segments per cell between 10 and 16. The average error is a good parameter to have an overall estimation of the quality of the reconstructed temperature map, especially when it assumes small values. On the other hand, it does not provide any information on the capability to reproduce the shape of the temperature map. For this reason, the coefficient of determination (R2) between the initial and calculated temperature maps was estimated and reported in Figure 10.

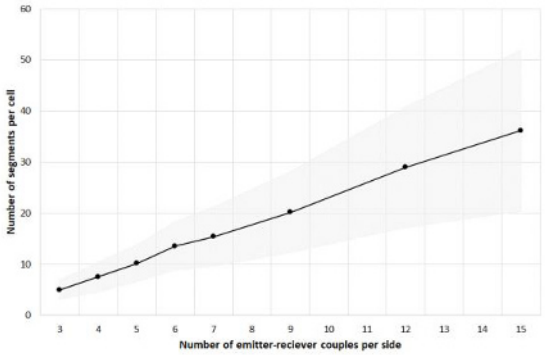

Figure 9. Number of segments per cell vs the number of ERCs per side.

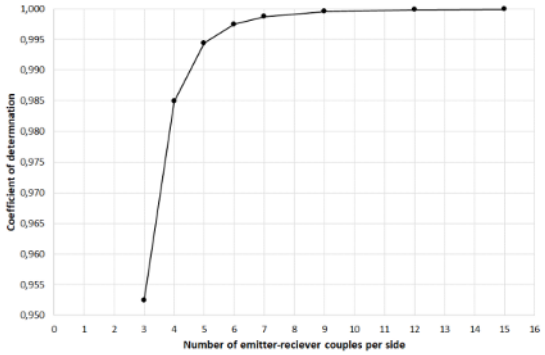

Figure 10. Coefficient of determination of temperature map vs the number of ERCs per side.

High values of the coefficient of determination have been achieved also for a small number of ERCs thus confirming a general capability of the technique to estimate the temperature map. By increasing the number of ERCs, the coefficient of determination rapidly increases and approaches values close to the unity. Again a number of ERCs between 5 and 7 seems the best solution.

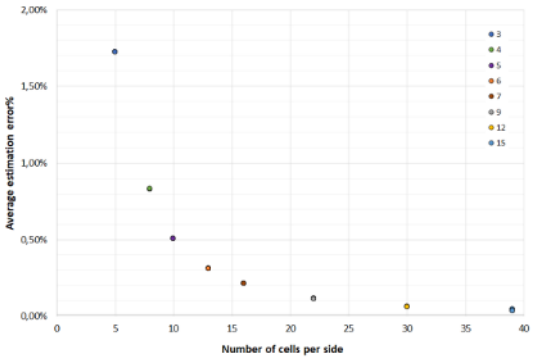

Figure 11. Repeatability of the estimation vs the number of ERCs per side.

The procedure to estimate the temperature map is based on an iterative approach that starts from a random distribution. A further investigation was performed to assess whether the final temperature estimation is

affected by the initial distribution or not. In other terms, the repeatability of the results was investigated by repeating the estimation of the temperature with the same setup for 15 consecutive times. The results are reported in Figure 11 in terms of the average relative estimation error (absolute values). The high repeatability of the procedure is clear, only for a very high number of ERCs a small increase in variability is observed. This probably due to the high number of cells that are used in that case.

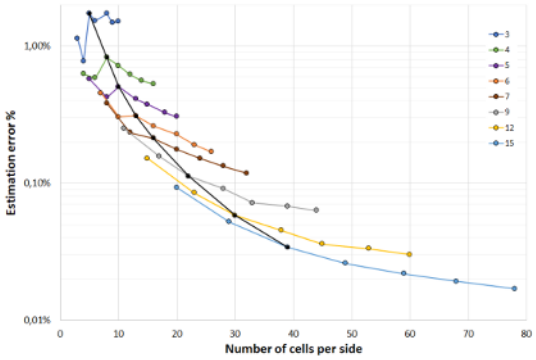

Figure 12. Temperature relative error vs the number of ERCs and cells per side.

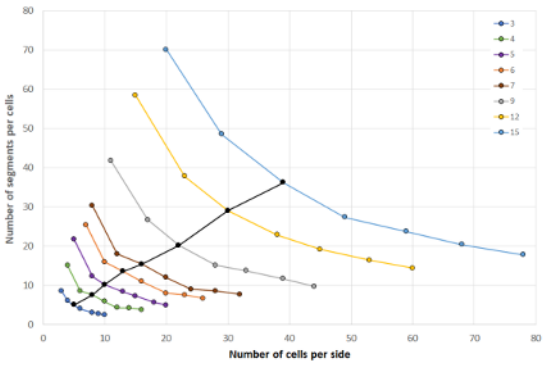

Figure 13. Number of segments per cell vs the number of ERCs and cells per side.

A further analysis on the measurement accuracy was performed by varying, for the same number of ERCs, the number of investigation cells. As the estimation procedure is not fully deterministic, the number of investigation cell might play a role in the determination of the temperature map. The results of this investigation are reported in Figure 12 and 13 where the average absolute relative error on the temperature estimation and the average number of segments per cell are reported for different combinations of ERCs and cell number per side. In more detail, for each ERCs per side, the number of cells considered was 0.5, 0.75, 1, 1.25, 1.50, 1.75 and 2 times that reported in Table 1. A black solid line connects the results achieved for a number of cells per side equal to that reported in Table 1. By increasing the number of cells, a reduction of the estimation error is achieved. This might be explained by considering that the by increasing the number of cells, also the resolution of the analysis increases. As only one value of temperature is associated to each cell, by increasing the number of investigation cells, a better description of the temperature distribution is possible. This benefit, is compensated by a reduction of the number of segments per cell. Thus, only a small increase in the number of investigation cells leads to significant improvements in the estimation accuracy.

4 Conclusion

Acoustic pyrometry is an interesting technique that can be used in several applications in the turbomachinery field. It does not require expensive instrumentation, allows the reconstruction of a temperature map and it is not influenced by the thermal inertia of the sensing element. On the other hand, several aspects should be taken into account to achieve a sufficient measurement accuracy. This study, which is a sort of preliminary investigation to a potential application of this technique, is focused on the analysis of the impact of the number of emitter-receiver-couples and investigation cells on the measurement results. A reference temperature distribution was assumed and the error in the temperature estimation due to different values of the number of ERCs was investigated. By increasing the number of ERCs the accuracy of the measurement increases. In any case, a good compromise between accuracy, simplicity of the setup and cost, seems to be a number of ERCs between 5 and 7. Further investigations will be devoted to investigate the reconstruction capability with temperature maps with increased complexity, the optimization of the grid size and the resilience to noise or other source of errors that might occur in an actual experimental context.

5 References

1. Venkateshan, SP, Shakkottai, PP, Kwack, EY, and Back LH, “Acoustic Temperature Profile Measurement Technique for Large Combustion Chambers”, ASME. J. Heat Transfer, 1989, 111(2), pp 461-466, doi:10.1115/1.3250699.
2. Bramanti, M, Salerno, EA, Tonazzini, A, Pasini, S, and Gray, A, “An acoustic pyrometer system for tomographic thermal imaging in power plant boilers”, in IEEE Transactions on Instrumentation and Measurement, 1996, vol. 45, no. 1, pp 159-167, doi: 10.1109/19.481329
3. Modlinski, N, Madejski, P, Janda, T, Szczepanek, K, and Kordylewski, W, “A validation of computational fluid dynamics temperature distribution prediction in a pulverized coal boiler with acoustic temperature measurement”, Energy, 2015, 92, pp 77-86
4. Sielschott, H, “Measurement of horizontal flow in a large scale furnace using acoustic vector tomography”, Flow Meas. Instrum., 1997, Vol. 8, Nos 3/4, pp. 191–197
5. De Silva, U, Bunce, RH, and Claussen, H, “Novel Gas Turbine Exhaust Temperature Measurement System”, ASME, Paper No. GT2013-95152, 2013, pp. V004T06A018; 8 pages, doi:10.1115/GT2013-95152
6. De Silva, U, Bunce, RH, Schmitt, JM, and Claussen, H, “Gas turbine exhaust temperature

measurement approach using time-frequency controlled sources", ASME, Paper No. GT2015-42139, 2015, pp. V006T05A001; 7 pages, doi:10.1115/GT2015-42139

7. Wassmer, D, Schuermans, B, Paschereit, C, and Moeck, JP, "An Acoustic Time-of-Flight Approach for Unsteady Temperature Measurements: Characterization of Entropy Waves in a Model Gas Turbine Combustor", ASME. J. Eng. Gas Turbines Power, 2016, doi:10.1115/1.4034542
8. Yan-Qin Li, and Huai-Chun Zhou, "Experimental study on acoustic vector tomography of 2-D flow field in an experiment-scale furnace", Flow Meas. and Instrum., 2006, Vol. 17, pp 113-122
9. Manuela Barth and Armin Raabe "Acoustic tomographic imaging of temperature and flow fields in air", 2011, Measurement Science and Technology, Volume 22, Number 3
10. Ziemann A, Arnold K and Raabe A "Acoustic tomography in the atmospheric surface layer", 1999, Ann. Geophys. 17 139–48